

Comparative EXAFS Investigation of Uranium(VI) and -(IV) Aquo Chloro Complexes in Solution Using a Newly Developed Spectroelectrochemical Cell

C. Hennig,* J. Tutschku, A. Rossberg, G. Bernhard, and A. C. Scheinost

Forschungszentrum Rossendorf, Institute of Radiochemistry,
P.O. Box 510119, 01314 Dresden, Germany

Received November 10, 2004

The coordination of the U(IV) and U(VI) ions as a function of the chloride concentration in aqueous solution has been studied by U L_{III}-edge extended X-ray absorption fine structure (EXAFS) spectroscopy. The oxidation state of uranium was changed in situ using a gastight spectroelectrochemical cell, specifically designed for the safe use with radioactive solutions. For U(VI) we observed the complexes $\text{UO}_2(\text{H}_2\text{O})_5^{2+}$, $\text{UO}_2(\text{H}_2\text{O})_4\text{Cl}^+$, $\text{UO}_2(\text{H}_2\text{O})_3\text{Cl}_2^0$, and $\text{UO}_2(\text{H}_2\text{O})_2\text{Cl}_3^-$ with $[\text{Cl}^-]$ increasing from 0 to 9 M, and for U(IV) we observed the complexes $\text{U}(\text{H}_2\text{O})_9^{4+}$, $\text{U}(\text{H}_2\text{O})_8\text{Cl}^{3+}$, $\text{U}(\text{H}_2\text{O})_6\text{Cl}_2^{2+}$, and $\text{U}(\text{H}_2\text{O})_5\text{Cl}_3^+$. The distances in the U(VI) coordination sphere are $\text{U}-\text{O}_{\text{ax}} = 1.76 \pm 0.02 \text{ \AA}$, $\text{O}_{\text{eq}} = 2.41 \pm 0.02 \text{ \AA}$, and $\text{U}-\text{Cl} = 2.71 \pm 0.02 \text{ \AA}$; the distances in the U(IV) coordination sphere are $\text{U}-\text{O} = 2.41 \pm 0.02 \text{ \AA}$ and $\text{U}-\text{Cl} = 2.71 \pm 0.02 \text{ \AA}$.

Introduction

For the disposal of nuclear waste in geological salt formations the complexation of uranium in concentrated chloride solutions is of great interest since it may considerably enhance actinide mobility. In oxygen-poor subsurface environments, U(VI) is likely to be reduced by microbial activity^{1–4} or by corroding nuclear waste storage containers.^{5–7} The reduction of U(VI) to U(IV) is assumed to retard uranium migration by precipitation of uraninite. However, formation of U(IV) chloride complexes could prevent uraninite precipitation and keep U(IV) mobile.

Comprehensive reviews of thermodynamic data have been reported on U(VI) complexes: a weighted linear regression, using experimental values from different references, yields

stability constants of $\log \beta_1^0 = 0.17 \pm 0.02$ and $\log \beta_2^0 = -1.1 \pm 0.02$ for the reaction $\text{UO}_2^{2+} + n\text{Cl}^- \rightleftharpoons \text{UO}_2\text{Cl}_n^{2-n}$.^{8,9} A wide scattering of experimental data accounts for difficulties to determine the thermodynamic parameters of the weak uranium chloride complexes. Formation constants $\log \beta_n^0$ for species with $n > 2$ have not been published so far. High chloride concentrations are required to replace H_2O molecules in the hydration sphere by Cl^- . Investigations of ligation effects at high chloride concentrations using Raman spectroscopy indicated a linear correlation between the frequency of the uranyl symmetrical stretching vibration ν_1 and the number of equatorially coordinated Cl atoms.¹⁰ From this correlation the species UO_2Cl^+ , UO_2Cl_2^0 , UO_2Cl_3^- , $\text{UO}_2\text{Cl}_4^{2-}$, and $\text{UO}_2\text{Cl}_5^{3-}$ were deduced in the concentration range 3–22 M $[\text{Cl}^-]$. UV–Vis spectroscopy shows significant spectral features which allowed to discriminate the species UO_2^{2+} , UO_2Cl^+ , and UO_2Cl_2^0 quantitatively.^{11,12} Allen et al.¹³ recently investigated the structure of U(VI) complexes in aqueous chloride solutions by EXAFS spec-

* Author to whom correspondence should be addressed. E-mail: hennig@esrf.fr. Fax: +33 (0)476 88 2505.

- (1) Lovley, D. R.; Phillips, J. P.; Gorby, Y. A.; Landa, E. R. *Nature* **1991**, *350*, 413–416.
- (2) Spear, J. R.; Figueroa, L. A.; Honeyman, B. D. *Appl. Environ. Microbiol.* **2000**, *66*, 3711–3721.
- (3) Suzuki, Y.; Kelly, S. D.; Kemner, K. M.; Banfield, J. F. *Appl. Environ. Microbiol.* **2003**, *69*, 1337–1346.
- (4) Fredrickson, J. K.; Zachara, J. M.; Kennedy, D. W.; Duff, M. C.; Gorby, Y. A.; Li, S. W.; Krupka, K. M. *Geochim. Cosmochim. Acta* **2000**, *64*, 3085–3098.
- (5) Duff, M.; Urbanik-Coughlin, J.; Hunter, D. B. *Geochim. Cosmochim. Acta* **2002**, *66*, 3533–3547.
- (6) Bruno, J.; De Pablo, J.; Duro, L.; Figuerola, E. *Geochim. Cosmochim. Acta* **1995**, *59*, 4113–4123.
- (7) Duro, L.; Rovira, M.; De Pablo, J.; El Aamrani, S.; Grivé, M.; Bruno, J. *Geochim. Cosmochim. Acta* **2004**, *68*, A497.

- (8) Grenthe, I.; Fuger, J.; Konings, R. J. M.; Lemire, R. J.; Muller, A. B.; Nguyen-Trung, C.; Wanner, H. In *Chemical Thermodynamics of Uranium*; Wanner, H., Forest, I., Eds.; Elsevier Science Publishers: Amsterdam, 1992; p 192.
- (9) Guillaumont, R.; Fanghänel, T.; Fuger, J.; Grenthe, I.; Neck, V.; Palmer, D. A.; Rand, M. H. In *Update on the chemical thermodynamics of uranium, neptunium, plutonium, americium and technetium*; Mompéan, F. J., Illemassene, M., Domenech-Orti, C., Ben Said, K., Eds.; Elsevier Science Publishers: Amsterdam, 2003; p 221.
- (10) Nguyen-Trung, C.; Begun, G. M.; Palmer, D. A. *Inorg. Chem.* **1992**, *31*, 5280–5287.

troscopy. For concentrations up to 14 M $[\text{Cl}^-]$, they observed the species $\text{UO}_2(\text{H}_2\text{O})_5^{2+}$, $\text{UO}_2(\text{H}_2\text{O})_x\text{Cl}^{1+}$, $\text{UO}_2(\text{H}_2\text{O})_x\text{Cl}_2$, and $\text{UO}_2(\text{H}_2\text{O})_x\text{Cl}_3^-$ with U–Cl distances varying from 2.71 to 2.73 Å.

In contrast to U(VI), little is known on chloride complexation by U(IV). The solubility of U(IV) in a 6 M NaCl solution decreases strongly at $\text{pH} > 3$.¹⁴ The formation constant according to the reaction $\text{U}^{4+} + n\text{Cl}^- \rightleftharpoons \text{UCl}_n^{4-n}$ extrapolated to an ionic strength $I = 0$ yields $\log \beta_1^0 = 1.72 \pm 0.13$.⁸ Only one experimental value is reported for $n = 2$ with a $\log \beta_2 = 0.06$ ($I = 2$ M).¹⁵

Considering the possible geochemical importance of U(IV) chloride complexes in salt formations on one hand and the uncertainty of complexation mechanisms and stability on the other hand, the intention of our study was to investigate these complexes over a range of chloride concentrations and by employing EXAFS spectroscopy for in situ speciation. Preliminary investigations revealed that even when oxygen exclusion was attempted, a considerable amount of U(IV) was oxidized too quickly to perform EXAFS measurements. To preserve the tetravalent oxidation state, we had to use an electrochemical cell for in situ EXAFS measurements. Spectroelectrochemistry is a well-known tool to investigate instable oxidation states.^{16,17} Due to the specific safety requirements for the handling of radioactive materials at the ESRF, we developed an electrochemical cell that is gastight and prevents the water decomposition typical for conventional models, since this could lead to an explosive mixture of H_2 and O_2 and to the subsequent release of radionuclides. The design of this spectroelectrochemical cell comprising two safety compartments and a special electrode arrangement is described. The use of this cell enabled us to study the transition from U(VI) to U(IV) in a closed system.

Experimental Section

Sample Preparation. UO_3 was obtained by heating $\text{UO}_2(\text{NO}_3)_2 \cdot n\text{H}_2\text{O}$ (Lachema) at 300 °C for 2 days. Two stock solutions of 0.1 M U were prepared by dissolving UO_3 either in 0.3 M HClO_4 (I) for the chloride-free sample or in 0.3 M HCl (II) for the chloride-containing samples. Four 0.01 M U(VI) aqueous solutions with chloride concentration of 0, 3, 6, and 9 M were prepared (Table 1). The chloride-free solution was prepared by 2.5 mL of the stock solution I, 1.75 mL HClO_4 , and water to obtain 25 mL of 0.01 M U solution. The chloride-containing solutions were prepared by 2.5 mL of the stock solution II and 1.75 mL of 1 M HCl in 20.75 mL of water. The chloride concentrations, given in Table 1, were adjusted by dissolving LiCl in the solutions.

- (11) Runde, W.; Neu, M. P.; Conradson, S. D.; Clark, D. L.; Palmer, P. D.; Reilly, S. D.; Scott, B. L.; Tait, C. D. *Mater. Res. Soc. Symp. Proc.* **1997**, 465, 693–703.
- (12) Paviet-Hartmann, P.; Lin, M. R. *Mater. Res. Soc. Symp. Proc.* **1999**, 556, 977–984.
- (13) Allen, P. G.; Bucher, J. J.; Shuh, D. K.; Edelstein, N. M.; Reich, T. *Inorg. Chem.* **1997**, 36, 6, 4676–4683.
- (14) Rai, D.; Felmy, A. R.; Sterner, S. M.; Moore, D. A.; Mason, M. J.; Novak, C. F. *Radiochim. Acta* **1997**, 79, 239–247.
- (15) Day, R. A., Jr.; Wilhite, R. N.; Hamilton, F. D. *J Am. Chem. Soc.* **1955**, 77, 3180–3182.
- (16) Soderholm, L.; Antonio, M. R.; Williams, C.; Wassermann, S. R. *Anal. Chem.* **1999**, 71, 4622–4628.
- (17) Antonio, M. R.; Soderholm, L.; Williams, C. W.; Blaudeau, J.-P.; Bursten, B. E. *Radiochim. Acta* **2001**, 89, 17–25.

Table 1. Sample Characterization

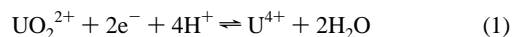
[U(VI)] ^a	[Cl [−]]	electrolyte	pH	U (V) ^b
0.01	0.0 ^c	0.1 M HClO_4	0.89	−0
0.01	3.0	0.1 M HCl	0.24	−80
0.01	6.0	0.1 M HCl	0.64	−80
0.01	9.0	0.1 M HCl	1.61	−80

^a Concentration in $\text{mol} \cdot \text{L}^{-1}$. ^b Potential for reduction vs Ag/AgCl. ^c This solution contains 0.02 M LiCl to activate the anode.

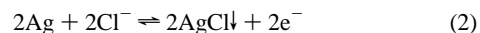
Electrochemistry. A drawing of the spectroelectrochemical cell is shown in Figure 1. The cell body consists of chemically resistant material (poly(tetrafluoroethylene) or poly(vinylidene fluoride)) and is sealed by two independent cover plates using rubber gaskets. These cover plates serve as double confinement against radionuclide release. Each cover plate contains six gastight connectors for cables and electrodes. Two X-ray windows were machined directly into the cell walls to avoid additional sealing. The windows are 20 mm apart from each other to allow sufficient X-ray transmission through the chloride solution and to achieve with 0.01 M U an edge jump of 0.3 at the U L_{III}-edge. The liquid volume of 10 mL was agitated by a magnetic stirrer.

All miniaturized electrodes and sensors were machined by KSI Mainsberg¹⁸ and were used in combination with a potentiostat (model PGU 20V-100mA).

The working electrode (cathode) was a Pt gauze. The electrochemical reduction of U(VI) to U(IV) involves an electron transfer and a chemical reaction transforming the *trans*-dioxo cation. The reaction at the cathode was



The counter electrode (anode) was an Ag wire. The Ag wire was dissolved and precipitated as silver chloride:



The dissolved Ag^+ ions were in equilibrium with solid AgCl, and the potential of the electrode was then determined by the solubility

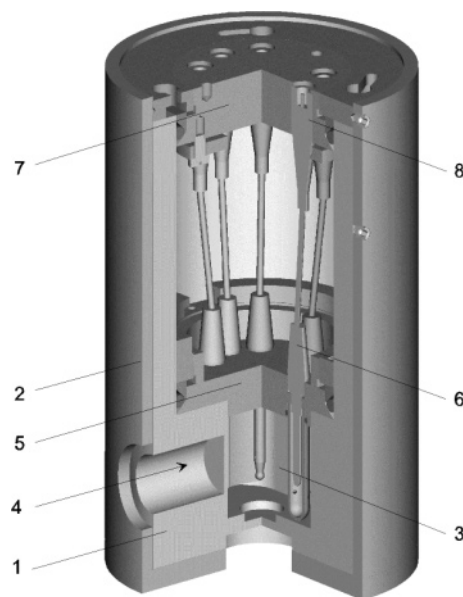


Figure 1. Drawing of the spectroelectrochemical cell: (1) cell body of chemically resistant material; (2) stainless steel housing; (3) space for the sample solution; (4) X-ray window; (5) inner cover plate (first compartment); (6) electrode; (7) outer cover plate (second compartment); (8) electrical connector.

constant of the precipitate. At the experimental conditions chosen, the electrochemical potential was always far away from the decomposition potential of water. To avoid a high polarization of the cell, no diaphragm was used. The reduction of 0.01 mol of U(VI) to U(IV) at the cathode was accompanied by a decrease in the chloride concentration due to the precipitation of 0.02 mol of AgCl. The resulting reduction of the chloride concentration was small in comparison to the chloride concentration of the 3, 6, and 9 M $[\text{Cl}^-]$ samples. To enforce the anode reaction in the nominally 0 M $[\text{Cl}^-]$ solution, 0.02 mol of LiCl was added. In both cases we did not expect an influence on speciation due to the low stability constants of the uranium chloride complexes. The Ag/AgCl potential was used as reference. The temperature of the solution was measured with a Pt thermocouple. Current–potential measurements were applied to gain redox potentials of the U(VI):U(IV) couple¹⁹ and appropriate potentials for the reduction process (Table 1). In preliminary experiments the completeness of reduction was verified by UV–vis spectroscopy. Above 4 M $[\text{Cl}^-]$, U(IV) was stable for several days. Therefore, only the EXAFS measurements of samples with 0 and 3 M $[\text{Cl}^-]$ were performed in the spectroelectrochemical cell by applying a constant reduction potential for 6 h. During the reduction process XANES measurements were performed in situ to monitor the actual oxidation state. To reduce the X-ray absorption due to high chloride concentrations, the samples with 6 and 9 M $[\text{Cl}^-]$ were reduced electrochemically and then transferred to polyethylene vials with 8 mm diameter. LiCl was used as electrolyte instead of NaCl to reduce the background absorption for the EXAFS spectra.

EXAFS Data Acquisition and Analysis. EXAFS measurements were carried out on the Rossendorf Beamline²⁰ at the European Synchrotron Radiation Facility (ESRF) under dedicated ring conditions (6.0 GeV, 200 mA). The monochromator equipped with a Si(111) double-crystal was used in channel-cut mode. Higher harmonics were rejected by two Pt coated mirrors. The first mirror collimates the X-ray beam onto the monochromator crystal, and the second mirror focuses the beam vertically to the sample. The vertical width of the secondary slit was 1.0 mm. Uranium L_{III}-edge spectra were collected in transmission mode using argon-filled ionization chambers at ambient temperature and pressure. Data were collected in equidistant k -steps of 0.05 \AA^{-1} across the EXAFS region. Three scans were recorded for each sample and then averaged. An Y metal foil (first inflection point at 17 038 eV) was used for energy calibration. The U L_{III} threshold energy, $E_{k=0}$, was defined for U(VI) and U(IV) as 17 185 eV. EXAFS data were extracted from the raw absorption spectra by standard methods including a spline approximation for the atomic background using the program EXAFSPAK.²¹ Theoretical phase and amplitude functions were calculated with FEFF 8.2.²² For U(VI), single and multiple scattering paths were calculated on the basis of the structure of $\text{Li}(\text{H}_2\text{O})_2[(\text{UO}_2)_2\text{Cl}_3(\text{O})(\text{H}_2\text{O})]^{23}$ and a hypothetical cluster for $\text{UO}_2(\text{H}_2\text{O})_5$; for U(IV) the structures of UCl_4^{24} and $\text{U}(\text{H}_2\text{O})_4(\text{SO}_4)_2^{25}$

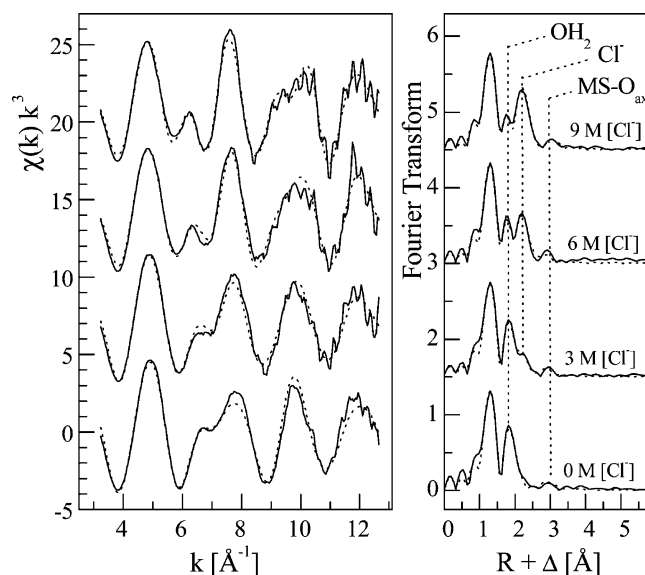


Figure 2. U L_{III}-edge k^3 -weighted EXAFS data (left) and corresponding Fourier transforms (right) taken over $k = 3.2\text{--}12.7 \text{ \AA}^{-1}$ for UO_2^{2+} as a function of $[\text{Cl}^-]$: experimental data (line); theoretical curve fit (dots).

were used. Due to increasing noise levels at higher k -range, data analysis was restricted to the k -range $3.2\text{--}12.7 \text{ \AA}^{-1}$ for U(VI) and to $3.2\text{--}9.6 \text{ \AA}^{-1}$ for U(IV). The distance resolution, $\Delta R = \pi/2\Delta k$, was 0.17 and 0.25 \AA for U(VI) and U(IV), respectively. This relatively narrow data range did not limit the data analysis up to a radial distance of 3 \AA , the maximum distance relevant for this study. The amplitude reduction factor, S_0^2 , was defined as 0.9 in the FEFF calculation and fixed to that value in the data fits. In all fits the coordination number of the uranyl oxygen atoms (O_{ax}) was held constant at 2. The 2-fold degenerated 4-legged multiple-scattering path $\text{U}\text{--}\text{O}_{\text{ax}1}\text{--}\text{U}\text{--}\text{O}_{\text{ax}2}$ was included in the curve fit by constraining its Debye–Waller factor and its effective path length to twice the values of the corresponding, freely fitted $\text{U}\text{--}\text{O}_{\text{ax}}$ single-scattering path.²⁶ The fitted energy shift parameter, ΔE_0 , was linked for all shells. In addition to conventional shell fit, which is often unable to differentiate between multiple coexisting species, EXAFS analysis was complemented by factor analysis including iterative target transformation using the program ITFA.²⁷ The data analysis comprises three steps: (i) decomposition of the experimental spectra into abstract spectra (factors) by factor analysis; (ii) transformation of the abstract spectra into real spectra using relative concentrations as constraints by iterative target transformation; (iii) standard shell fitting of the real spectra to gain structural parameters of the limiting structural units.

Results and Discussion

U(VI) Chloride Complexation. U L_{III}-edge k^3 -weighted EXAFS spectra and the corresponding Fourier transforms (FT) are shown in Figure 2. Structural results of the standard EXAFS shell fitting including phase correction are summarized in Table 2. The FT of the UO_2^{2+} aquo ion (sample

(18) Kurt-Schwabe-Institut für Mess und Sensortechnik e.V. Meinsberg, Fabrikstrasse 69, D-04720 Ziegra-Knobelsdorf, Ortsteil Meinsberg, Germany.

(19) Kihara, S.; Yoshida, Z.; Aoyagi, H.; Maeda, K.; Shirai, O.; Katatsuji, Y.; Yoshida, Y. *Pure Appl. Chem.* **1999**, *71*, 1771–1807.

(20) Matz, W.; Schell, N.; Bernhard, G.; Prokert, F.; Reich, T.; Claussner, J.; Oehme, W.; Schlenk, R.; Dienel, S.; Funke, H.; Eichhorn, F.; Betzl, M.; Pröhl, D.; Strauch, U.; Hüttig, G.; Krug, H.; Neumann, W.; Brendler, V.; Reichel, P.; Dencke, M. A.; Nitsche, H. *J. Synchrotron Radiat.* **1999**, *6*, 1076–1085.

(21) George, G. N.; Pickering, I. J. *EXAFSPAK, a suite of computer programs for analysis of X-ray absorption spectra*; Stanford Synchrotron Radiation Laboratory: Stanford, CA, 2000.

(22) Ankudinov, A. L.; Ravel, B.; Rehr, J. J.; Conradson, S. D. *Phys. Rev.* **1998**, *B58*, 7565–7576.

(23) Bean, A. C.; Xu, Y.; Danis, J. A.; Albrecht-Schmitt, T. E.; Scott, B. L.; Runde, W. *Inorg. Chem.* **2002**, *41*, 6775–6779.

(24) Schleid, T.; Meyer, G.; Morss, G. R. *J. Less-Common Met.* **1987**, *132*, 69–77.

(25) Kierkegaard, P. *Acta Chim. Scand.* **1956**, *10*, 599–610.

(26) Hudson, E. A.; Rehr, J. J.; Bucher, J. J. *Phys. Rev. B* **1995**, *52*, 13815–13826.

(27) Rossberg, A.; Reich, T.; Bernhard, G. *Anal. Bioanal. Chem.* **2003**, *376*, 631–638.

Table 2. EXAFS Structural Parameters of U(VI) Aquo and Chloro Complexes

	U–O _{ax}			U–O _{eq}		U–Cl		ΔE_0 (eV)
	<i>R</i> (Å)	<i>N</i>	σ^2 (Å ²)	<i>R</i> (Å)	<i>N</i>	<i>R</i> (Å)	<i>N</i>	
0 M [Cl [−]]	1.76	2 ^a	0.0014	2.41	5.2			2.1
				1st Model				
3 M [Cl [−]]	1.76	2 ^a	0.0017	2.41	3.9	2.73	1.0	2.5
6 M [Cl [−]]	1.76	2 ^a	0.0011	2.42	1.7	2.73	2.3	0.9
9 M [Cl [−]]	1.76	2 ^a	0.0014	2.51	1.4	2.74	2.7	0.1
				2nd Model				
3 M [Cl [−]]	1.76	2 ^a	0.0017	2.41 ^a	3.9	2.71 ^a	1.1	2.1
6 M [Cl [−]]	1.76	2 ^a	0.0011	2.41 ^a	1.7	2.71 ^a	2.3	0.3
9 M [Cl [−]]	1.76	2 ^a	0.0014	2.41 ^a	0.7	2.71 ^a	3.1	−1.5
				ITFA-Derived Limiting Structural Units				
UO ₂ O _x	1.76	2 ^a	0.0014	2.41	5.2			2.1
UO ₂ Cl _y	1.76	2 ^a	0.0010			2.71	5.1	−3.3

^a Value fixed during the fit procedure. Errors in distances *R* are ± 0.02 Å; errors in coordination numbers *N* are $\pm 15\%$. The Debye–Waller factor σ^2 was held constant for the shells U–O_{eq}, $\sigma^2 = 0.0075$ Å², and U–Cl, $\sigma^2 = 0.0050$ Å². A *k* range of 3.2–12.7 Å^{−1} was used.

0 M [Cl[−]]) shows two peaks which arise from two O_{ax} at 1.76 ± 0.02 Å and 5 equatorial oxygen atoms (O_{eq}) at 2.41 ± 0.02 Å. This result is in agreement with structural parameters obtained previously for the UO₂²⁺ aquo ion in HClO₄ electrolyte.^{28–31}

The FTs of the chloride solutions show an additional peak at a distance of 2.73 ± 0.02 Å indicative of Cl in the first coordination sphere. The intensity of this peak increases with increasing chloride concentration. It should be noted that EXAFS analysis reflects only the average coordination and is not able to differentiate between coexisting species if the bond lengths are equal. Therefore, in the fit procedure the bond lengths of possible solution species comprising UO₂(H₂O)₅²⁺ and UO₂(H₂O)_{5−*n*}Cl_{*n*}^{2−*n*} are averaged to a common radial distribution. The Debye–Waller factors, σ^2 , were fixed for the EXAFS fit procedure to make the relation between O_{eq} and Cl comparable and to avoid the correlation problems between *N* and σ^2 . For the U–O_{eq} shell a Debye–Waller factor of 0.0075 Å² was estimated from UO₂(H₂O)₅²⁺ in 0.1 M HClO₄ solution. The Debye–Waller factor for the U–Cl shell was fixed at 0.0050 Å² as obtained from UO₂Cl₄^{2−}.¹³ With increasing [Cl[−]] the coordination number *N*_{Cl} increases from 1.0 to 2.7 and the coordination number *N*_{O_{eq}} decreases from 3.9 to 1.4. These fit results indicate that even in a high concentration of 9 M [Cl[−]], a part of the equatorial shell consists of H₂O. The U–Cl distance remains nearly constant at 2.73 ± 0.02 Å for all samples. The U–O_{eq} distance is 2.41 ± 0.02 Å for the samples up to 6 M [Cl[−]] but increases to 2.51 ± 0.02 Å at 9 M [Cl[−]]. This observation agrees with that of Allen et al.¹³ An investigation of comparable crystal structures shows that the pure U(VI) chloride complex has 4 Cl ligands in the equatorial shell.^{32,33} If one H₂O molecule is added to the equatorial shell, the

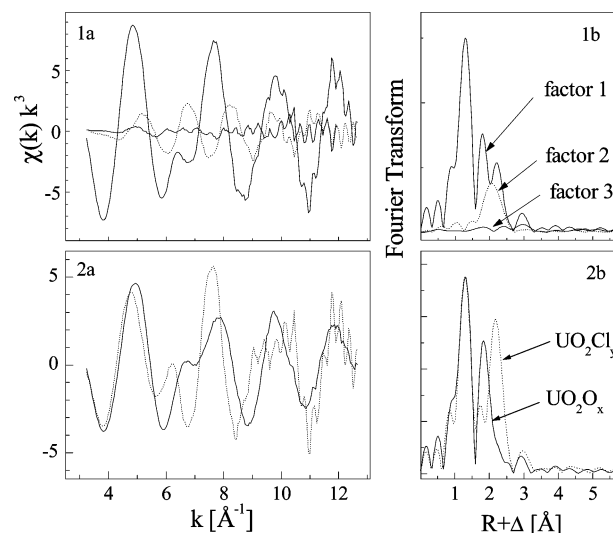


Figure 3. First three isolated abstract spectra of the U(VI)/Cl series (1a) and their corresponding Fourier transforms (1b). Spectra of limiting structural units (2a) and their corresponding Fourier transforms (2b).

coordination number increases from 4 to 5^{34–36} and remains 5 until the ion exchange is completed. Crystal structures with a coordination $N_{\text{Cl}} + N_{\text{Oeq}} = 4$, which could be compared to the 1st fit model of the 9 M [Cl[−]] sample, are not known.

Wasserman et al.³⁷ showed that the standard EXAFS analysis of U(VI) aquo chloro complexes has some inherent limitations which can be overcome by model-independent statistical methods. Hence, the four spectra shown in Figure 2 were analyzed with factor analysis. Three main factors representing the O_{eq} atoms at 2.41 Å and at 2.51 Å as well as the Cl shell were expected. The experimental spectra are decomposed by factor analysis in a set of abstract spectra (without direct physical meaning). Figure 3.1 shows the decomposition results. The first two abstract spectra have large amplitudes and generate the main features in the Fourier

- (28) Wahlgren, U.; Moll, H.; Grenthe, I.; Schimmelpfennig, B.; Maron, L.; Vallet, V.; Groppen, O. *J. Phys. Chem.* **1999**, *103*, 8257–8264.
 (29) Vallet, V.; Wahlgren, U.; Schimmelpfennig, B.; Moll, H.; Szabó, Z.; Grenthe, I. *Inorg. Chem.* **2001**, *40*, 3516–3525.
 (30) Thompson, H. A.; Brown, G. E., Jr.; Parks, G. A. *Am. Mineral.* **1997**, *82*, 483–496.
 (31) Sémon, L.; Boehme, C.; Billard, I.; Hennig, C.; Lützenkirchen, K.; Reich, T.; Rossberg, A.; Rossini, I.; Wipff, G. *Chem. Phys. Chem.* **2001**, *2*, 591–598.
 (32) Tutov, A. G.; Plakhtii, V. P.; Usov, O. A.; Bublyayev, R. A.; Chernenkov, Y. P. *Kristallografiya* **1991**, *36*, 1135–1138.

- (33) Anson, C. E.; Al-Jowder, O.; Upali, A.; Jayasooriya, U. A.; Powell, A. K. *Acta Crystallogr. C* **1996**, *52*, 279–281.
 (34) Debets, P. C. *Acta Crystallogr. B* **1968**, *24*, 400–402.
 (35) Taylor, J. C.; Wilson, P. W. *Acta Crystallogr. B* **1973**, *29*, 1073–1076.
 (36) Taylor, J. C.; Wilson, P. W. *Acta Crystallogr. B* **1974**, *30*, 169–175.
 (37) Wasserman, S. R.; Allen, P. G.; Shuh, D. K.; Bucher, J. J.; Edelstein, N. M. *J. Synchrotron Radiat.* **1999**, *6*, 284–286.

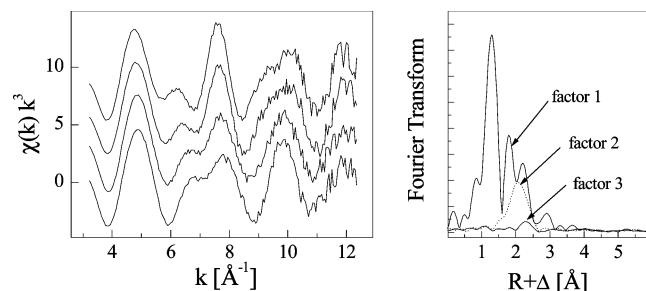
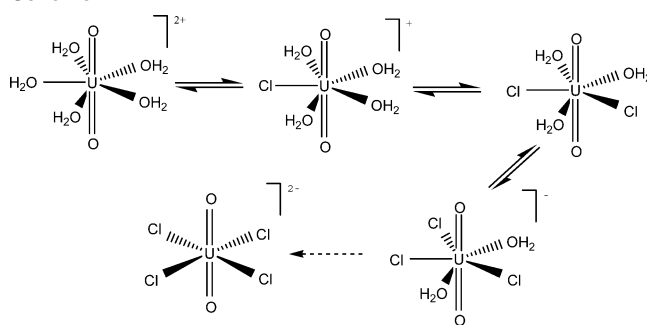


Figure 4. Model EXAFS spectra with artificial noise created with the fit parameters of the 1st model, i.e., including an additional elongated U–O_{eq} distance (left), and the Fourier transforms of the abstract spectra derived by ITFA (right).

transform. The amplitude of the third abstract spectrum does not rise above the experimental noise level. Hence, all meaningful spectral features are reproduced by only two factors. Assuming that one factor arises from the structural unit UO₂O_x and the other from the structural unit UO₂Cl_y, the quantitative relation between O and Cl obtained from the 9 M [Cl[−]] sample can be used to transform the two abstract spectra into real spectra by iterative target transformation. These real spectra represent the limiting structural units with only O or with only Cl in the equatorial coordination shell (Figure 3.2). The limiting structural units may represent real species, as is the case for the fully hydrated UO₂O_x species. In the case of UO₂Cl_y, however, the limiting structural unit does not represent a real species but is a hypothetical coordination extracted from the spectral contribution of U–Cl and U–O backscattering pairs in mixed-coordination spheres. A shell fit of these limiting structural units yielded a bond length of 2.71 Å for U–Cl, a bond length of 2.41 Å for U–O_{eq}, and an approximate coordination number of 5 for both shells (Table 2, bottom rows). Note that if a second O_{eq} shell with a longer distance of 2.51 Å existed in part of the spectra, one would expect that a third factor is required to reproduce the spectra and that the Fourier transform of this factor shows a peak between those arising from O_{eq} and Cl atoms, i.e., at approximately 2 Å (uncorrected for phase shift). The absence of such a third factor with a meaningful frequency in the expected range suggests that an additional U–O_{eq} bond length of 2.51 Å does not exist.

To verify that ITFA would be sensitive enough to detect the possibly weak contribution of a second O_{eq} shell, we generated a set of model EXAFS spectra on the basis of our first shell fitting results (1st model in Table 2, dotted lines in Figure 2), i.e., including the U–O_{eq} distance of 2.51 Å (Figure 4, left). To make the calculated spectra comparable to experimental spectra, artificial noise was added. This set of calculated model spectra was then decomposed with ITFA in a set of abstract spectra, the same way as it was done before with the experimental spectra. The Fourier transform of the third abstract spectrum clearly reveals the expected peak due to the additional, longer U–O_{eq} distance (Figure 4, right). This means that such an elongated U–O_{eq} distance would be detectable by ITFA. Therefore, this sensitivity test clearly demonstrates that such an elongated U–O_{eq} distance does not exist. The most likely explanation for its appearance

Scheme 1



in shell-fitting attempts is that the strongly overlapping frequencies cannot be properly resolved, hence, that it is a mere fitting artifact.

The distances U–Cl (2.71 Å) and U–O_{eq} (2.41 Å) derived from the limiting structural units were now used as constraints for a 2nd fit model. The resulting *N*_{O_{eq}} is slightly lower and *N*_{Cl} is higher than in the 1st model, while the sum *N*_{Cl} + *N*_{O_{eq}} remains close to 4. This is in contrast to factor analysis, where the two limiting structural units had 5 H₂O or 5 Cl ligands. The contradictory results of both methods may be resolved as follows. In uranyl structures, the U–O and U–Cl distances become generally shorter if the equatorial coordination number is reduced from 5 to 4.³⁸ For example in UO₂AsO₄[−] (*N*_{O_{eq}} = 4) the U–O_{eq} bond length is 2.282 Å³⁹ and in UO₂Cl₄^{2−} (*N*_{Cl} = 4) the U–Cl bond length is 2.671 Å.⁴⁰ In good agreement, the fully chlorinated U(VI) species with *N*_{Cl} = 4 obtained from a 10 M [Cl[−]] solution by Dowex anion-exchange resin shows a U–Cl distance of 2.67 Å.¹³ Since we do not observe such a bond shortening, we assume that the result from factor analysis with iterative target transformation, i.e., a coordination number of 5 for all aquo chloro complexes related with bond lengths for U–Cl = 2.71 Å and U–O_{eq} = 2.41 Å, is correct. In conclusion, the structural parameters extracted by EXAFS suggest the species UO₂(H₂O)₄Cl⁺, UO₂(H₂O)₃Cl₂⁰, and UO₂(H₂O)₂Cl₃[−] according to Scheme 1. An exclusive Cl[−] coordination in the equatorial shell, as in UO₂Cl₄^{2−}, was not observed within the applied experimental conditions.

U(IV) Chloride Complexation. Figure 5 shows the EXAFS spectra after reduction of U(VI) to U(IV). The corresponding EXAFS fit results are summarized in Table 3. In noncomplexing perchloric acid (sample 0 M [Cl[−]]), the aquo ion has 8.7 spherically arranged O atoms at a distance of 2.41 Å. This coordination number is less than that of 10 previously determined by EXAFS⁴² but is larger

(38) Burns, P. C.; Miller, M. L.; Ewing, R. C. *Can. Mineral.* **1996**, *34*, 845–880.

(39) Hennig, C.; Reck, G.; Reich, T.; Rossberg, A.; Kraus, W.; Sieler, J. *Z. Kristallogr.* **2003**, *218*, 37–45.

(40) Watkin, D. J.; Denning, R. G.; Prout, K. *Acta Crystallogr. C* **1991**, *47*, 2517–2519.

(41) Conradson, S. D.; Abney, K. D.; Begg, B. D.; Brady, E. D.; Clark, D. L.; den Auwer, C.; Ding, M.; Dorhout, P. K.; Espinosa-Faller, F. J.; Gordon, P. L.; Haire, R. G.; Hess, N. J.; Hess, R. F.; Keogh, D. W.; Lander, G. H.; Lupinetti, A. J.; Morales, L. A.; Neu, M. P.; Palmer, P. D.; Paviet-Hartmann, P.; Reilly, S. D.; Runde, W. H.; Tait, C. D.; Veirs, D. K.; Wastin, F. *Inorg. Chem.* **2004**, *43*, 116–131.

(42) Moll, H.; Denecke, M. A.; Jalilvand, F.; Sandström, M.; Grenthe, I. *Inorg. Chem.* **1999**, *38*, 1795–1799.

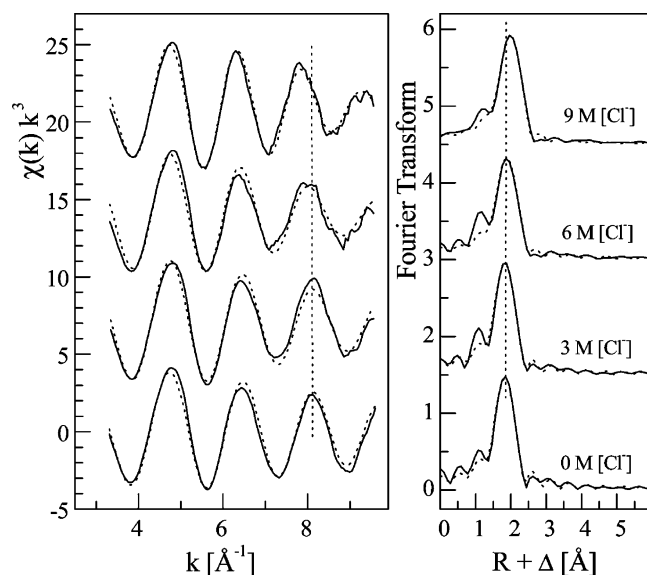


Figure 5. U L_{III} -edge k^3 -weighted EXAFS data (left) and corresponding Fourier transforms (right) taken over $k = 3.2$ – 9.6 \AA^{-1} for U(IV) as a function of $[\text{Cl}^-]$: experimental data (line); theoretical curve fit (dots).

Table 3. EXAFS Structural Parameters of U(IV) Aquo and Chloro Complexes

	U–O		U–Cl		ΔE_0 (eV)
	R (Å)	N	R (Å)	N	
0 M $[\text{Cl}^-]$	2.41	8.7			–2.1
		1st Model			
3 M $[\text{Cl}^-]$	2.41	8.5	2.77	0.3	–1.3
6 M $[\text{Cl}^-]$	2.43	7.6	2.76	0.8	–0.4
9 M $[\text{Cl}^-]$	2.44	6.1	2.73	2.1	–0.7
		2nd Model			
3 M $[\text{Cl}^-]$	2.41 ^a	8.5	2.71 ^a	0.3	–1.3
6 M $[\text{Cl}^-]$	2.41 ^a	6.7	2.71 ^a	1.4	–1.2
9 M $[\text{Cl}^-]$	2.41 ^a	5.2	2.71 ^a	2.7	–3.3
	ITFA-Derived Limiting Structural Units				
$\text{U}^{\text{IV}}\text{O}_x$	2.41	8.7			–2.1
$\text{U}^{\text{IV}}\text{Cl}_y$			2.71	7.7	–3.3

^a Value fixed during the fit procedure. Errors in distances R are $\pm 0.02 \text{ \AA}$; errors in coordination numbers N are $\pm 15\%$. The Debye–Waller factor σ^2 was held constant for the shells U–O_{eq}, $\sigma^2 = 0.0070 \text{ \AA}^2$, and U–Cl, $\sigma^2 = 0.0050 \text{ \AA}^2$. A k range of 3.2 – 9.6 \AA^{-1} was used.

than the coordination number of 8 determined by large-angle X-ray scattering.^{43,44} Coordination numbers of 8–9 prevail in crystal structures.⁴⁵ Finally, a coordination number of 9 was estimated with relativistic density functional theory for U(IV) in aqueous solution.⁴⁶

With increasing $[\text{Cl}^-]$ the dominant FT peak shifts to higher R values indicating the successive replacement of H_2O by Cl^- in the first coordination sphere. The σ^2 value of the U–O shell was fixed in the fit to 0.0070 \AA^2 , as obtained for the U(IV) aquo ion, and that of the U–Cl shell was fixed to 0.0050 \AA^2 assuming the same value as obtained for U(VI). The coordination number N_{Cl} increases from 0.3 to 2.1, the

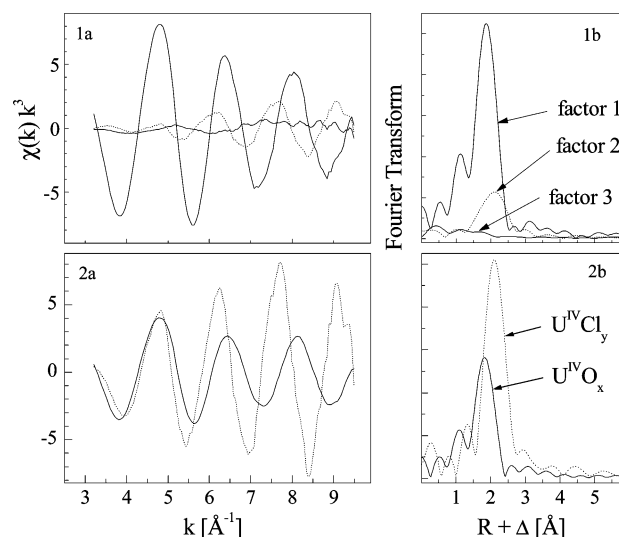


Figure 6. First three isolated abstract spectra of the U(IV)/Cl series (1a) and their corresponding Fourier transforms (1b). Spectra of the limiting structural units (2a) and their corresponding Fourier transforms (2b).

coordination number N_{O} decreases from 8.5 to 6.1, the U–O bond distances expand from 2.41 to 2.44 \AA , and the U–Cl bond distances are reduced from 2.77 to 2.73 \AA (1st model in Table 3).

To verify these differences of the bond lengths, factor analysis was again performed. As for U(VI), the decomposition results show that the four EXAFS spectra can be reproduced with only two factors, related to U–O and U–Cl backscattering contributions (Figure 6.1). A third factor shows a low-frequency EXAFS-like oscillation with a corresponding FT maximum at $R + \Delta = 0.5 \text{ \AA}$. Such a value is too short for a bond distance and is a typical artifact of the spline background removal.⁴⁷ The quantitative relation between O and Cl obtained from the 9 M $[\text{Cl}^-]$ sample was used to separate the real spectra of the limiting structural unit $\text{U}^{\text{IV}}\text{O}_x$ and $\text{U}^{\text{IV}}\text{Cl}_y$ with iterative target transformation (Figure 6.2). The shell fit results are given in the bottom rows of Table 3. The structural parameters of the $\text{U}^{\text{IV}}\text{O}_x$ shell are identical with the fit results of the 0 M $[\text{Cl}^-]$ spectrum, suggesting 9 water molecules in the first shell. On the basis of the results from factor analysis, the bond lengths of U–O and U–Cl were fixed in a subsequent two-shell fit to 2.41 and 2.71 \AA , respectively (2nd model). With increasing $[\text{Cl}^-]$, the coordination number $N_{\text{Cl}} + N_{\text{O}}$ decreases from 8.8 to 7.9. In good agreement, the limiting structural unit $\text{U}^{\text{IV}}\text{Cl}_y$ shows a coordination number of 7.7. Therefore, we assume that the aquo chloro shell in the 9 M $[\text{Cl}^-]$ solution comprises only 8 ligands. Although the absolute error in determining coordination numbers is high, the experimental standard deviation within a series of samples, prepared and measured under the same conditions, is expected to be much smaller and the decrease of the first-shell coordination number by 1 is most likely significant. This observation is in line with a mixed $N_{\text{Cl}} + N_{\text{O}}$ coordination of 7 or 8 in several crystal

(43) Pocev, S.; Johansson, G. *Acta Chem. Scand.* **1973**, *27*, 2146–2160.

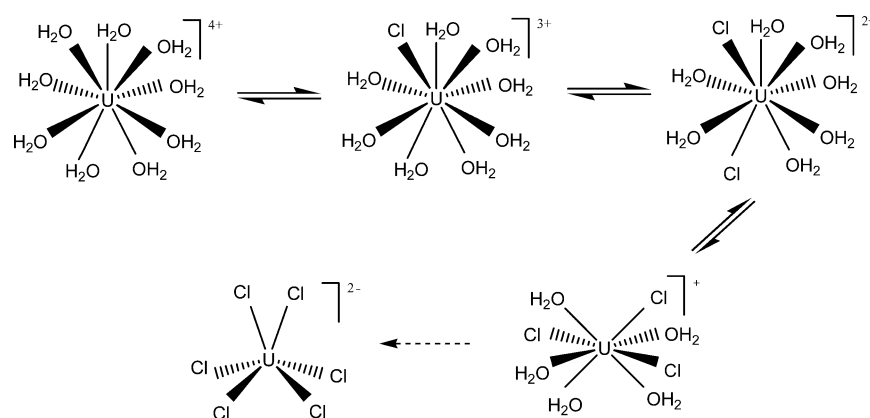
(44) Johansson, G. Structures of complexes in solution derived from X-ray diffraction measurements. In *Advances in Inorganic Chemistry*; Academic Press: London, 1992; Vol. 39.

(45) Clausen, K.; Hayes, W.; MacDonald, J. E.; Schnabel, P.; Hutchings, M. T.; Kjems, J. K. *High Temp. High Press.* **1983**, *15*, 383–390.

(46) Tsushima, S.; Tianxiao, Y. *Chem. Phys. Lett.* **2005**, *401*, 68–71.

(47) Teo, B. K. In *EXAFS: basic principles and data analysis*; Springer: Berlin, Heidelberg, Germany, 1986.

Scheme 2



structures.^{48,49} Exclusive coordination of U(IV) by Cl^- as in Cs_2UCl_6 yields a coordination number N_{Cl} of 6 related to a U–Cl distance of 2.62 Å.²⁴ The U–Cl distance of 2.71 Å, extracted from our samples by factor analysis, is longer than that observed for the UCl_6^{2-} species, hence, is rather indicative of a coordination number of approximately 8–9 $N_{\text{Cl}} + N_{\text{O}}$ ligands. In conclusion, the aquo chloro species derived from EXAFS measurements are identified as $\text{U}(\text{H}_2\text{O})_8\text{Cl}^{3+}$, $\text{U}(\text{H}_2\text{O})_6\text{Cl}_2^{2+}$, and $\text{U}(\text{H}_2\text{O})_5\text{Cl}_3^{3+}$ as shown in Scheme 2.

Concluding Remarks

The EXAFS measurements performed in aqueous chloride solutions demonstrate that both U(VI) and U(IV) form complexes with mixed aquo and chloro ligands. With increasing $[\text{Cl}^-]$ the coordination number of Cl increases stepwise. The ligands are coordinated in an inner-sphere fashion. An additional outer-sphere coordination could not be verified, since EXAFS measurement are not sensitive for the backscattering signals at $R + \Delta > 3$ Å under the used experimental conditions. Even with improved signal-to-noise ratio, the outer-sphere coordination would most likely be too disordered to be detectable.

U(VI) Aquo Chloro Complexes. For U(VI), conventional shell-fitting EXAFS analysis indicates that the U–O bond lengths increases from 2.41 to 2.51 Å with increasing $[\text{Cl}^-]$. This elongation was described for the first time by Allen et al.¹³ and was interpreted as a chemical effect due to the presence of chloride ions. We could verify this bond elongation by shell-fitting. However, decomposition of the spectra by factor analysis clearly demonstrated that the bond lengths remain invariant within ± 0.02 Å. The elongation observed with shell fitting is hence a fit artifact. Consequently, the influence of Cl on the U–O bond length seems to be weak.

Up to 9 M $[\text{Cl}^-]$, a decrease in the U(VI) coordination number $N_{\text{Cl}} + N_{\text{O}}$ from 5 to 4 can be excluded. This is in contrast to Pu(VI) aquo chloro complexes, where a reduction of the coordination number $N_{\text{Oeq}} + N_{\text{Cl}}$ from 5 to 4 was observed already during the second chlorination step.⁴¹

U(IV) Aquo Chloro Complexes. The obtained coordination of 9 H_2O for the U(IV) aquo species is in good agreement with results from relativistic density functional theory.⁴⁶ The coordination of U(IV) chloride complexes was not investigated up to now.⁹ We found that the combined coordination number $N_{\text{Cl}} + N_{\text{O}}$ decreases from 9 at low $[\text{Cl}^-]$ to 8 at 9 M $[\text{Cl}^-]$. For comparison, the chemically similar Np(IV) aquo chloro complexes show a more pronounced change of $N_{\text{Cl}} + N_{\text{O}}$ from 11 at 1 M $[\text{Cl}^-]$ to 8 at 10 M $[\text{Cl}^-]$.¹³

At the highest chloride concentration of 9 M, the obtained Cl coordination numbers of U(IV) and U(VI) are indicative of the species $\text{U}(\text{H}_2\text{O})_5\text{Cl}_3^{3+}$ and $\text{UO}_2(\text{H}_2\text{O})_2\text{Cl}_3^{2-}$, respectively. Although an increase in complexation strength might be expected by the reduction from U(VI) to U(IV), the number of coordinated Cl did not change at 9 M $[\text{Cl}^-]$. At lower $[\text{Cl}^-]$, however, the coordination numbers even decrease. Whether this effect is real or simply an effect of the lower statistical reliability of small Cl coordination numbers remains open.

On the basis of theoretical considerations, one might expect that with increasing N_{Cl} the effective charge of uranium decreases; hence, the U–Cl distance should slightly increase. However, we did not observe any changes of the bond lengths with increasing $[\text{Cl}^-]$ within the error limit of 0.02 Å.

The bond lengths for U–O (2.41 Å) and U–Cl (2.71 Å) are identical for U(VI) and U(IV). This suggests that, despite the difference in formal oxidation state, the effective ionic radii of U(VI) and U(IV) are similar, as has been pointed out before.⁵⁰

Acknowledgment. The EXAFS measurements were performed at the Rossendorf Beamline²⁰/ESRF. We thank D. Rettig and T. Reich (now University Mainz) for the technical development of a first version of the spectroelectrochemical cell and J. Claussner and D. Falkenberg for their support during the development of the final cell. The fruitful discussions with R. G. Denning and P. Paviet-Hartmann are gratefully acknowledged.

IC048422N

(48) Bernard-Rocherulle, P.; Louer, D.; Dacheux, N.; Brandel, V.; Genet, M. *J. Solid State Chem.* **1997**, *132*, 315–322.

(49) Levet, J. C.; Potel, M.; le Marouille, J. Y. *J. Solid State Chem.* **1980**, *32*, 287–302.

(50) Denning, R. G. Electronic structure and bonding in actinyl ions. In *Structure and Bonding*; Springer: Heidelberg, Germany, 1992; Vol. 79.